Sensors and Actuators A 303 (2020) 111700

Contents lists available at ScienceDirect

Sensors and Actuators A: Physical

journal homepage: www.elsevier.com/locate/sna

MEMS piezo-resistive force sensor based on DC sputtering deposited amorphous carbon films

Xin Ma[a,b,1], Xiaoshan Tong[a,1], Peng Guo[b], Yulong Zhao[a], Qi Zhang[a,*], Hanchao Li[b,d], Rende Chen[b], Aiying Wang[b,c,**]

[a] The State Key Laboratory for Mechanical Manufacturing Systems, Xi'an Jiaotong University, Xi'an, 710049, China
[b] Key Laboratory of Marine Materials and Related Technologies, Zhejiang Key Laboratory of Marine Materials and Protective Technologies, Ningbo Institute of Materials Technology and Engineering, Chinese Academy of Sciences, Ningbo, 315201, China
[c] Center of Materials Science and Optoelectronics Engineering, University of Chinese Academy of Sciences, Beijing, 100049, China
[d] School of Physical Science and Technology, ShanghaiTech University, Shanghai, 201210, China

ARTICLE INFO

Article history:
Received 6 August 2019
Received in revised form 7 October 2019
Accepted 26 October 2019
Available online 31 October 2019

Keywords:
Amorphous carbon film
Piezo-resistive effect
MEMS
Force sensor
Gauge factor

ABSTRACT

The rapid growing demand of micro-electromechanical system (MEMS) sensors brings an urgent need for high performance and low cost sensitive materials. In this work, amorphous carbon (a-C) film was in-situ deposited on silicon substrate as strain sensitive component using economical direct current (DC) magnetron sputtering process and the a-C sensor was systematically designed, fabricated and tested. By adjusting the negative bias voltage in the range of 0–400 V, the gauge factor (GF) of the a-C film was adjusted within the range of 3.3–6.9. What's more, the film's sp^2 cluster size played an important role in their piezo-resistive performance and conductivity, which illustrated the thick-film resistors (TFRs) theory. Additionally, CAFM results also supported the applying of TFRs theory in this work. Benefiting from the outstanding performance of a-C film, the MEMS force sensor, consisted a Wheatstone full-bridge with four a-C piezo-resistors, had a sensitivity of 9.8 μV/V/mN and non-linearity about 2.0% FS in the testing range of 0–210 mN, while it also showed a good repeatability. These investigations provided deeper insight into the piezo-resistive behavior of a-C film and contributed to the development of high performance and more economical sensitive materials for MEMS sensors.

© 2019 Elsevier B.V. All rights reserved.

1. Introduction

Amorphous carbon films (a-C) and hydrogenated amorphous carbon (a-C:H) films are widely used as protective material for their excellent properties, such as chemical inertness, high hardness, optical transparency and low frication coefficient [1]. Besides, combining with their outstanding electrical properties and high stress sensitivity [2–4], a-C films are considered as one promising sensitive material used in the MEMS sensors.

Compared with the most widely used silicon-based piezo-resistive material, gauge factor (GF) of a-C is in the same level or even an order of magnitude higher. According to previous reports, the GF of a-C or a-C:H can range from 50 to 1200 [5,6], depending on the component and preparation process of the films. In addition, with the introduction of a third element, the resistivity of a-C film can show weak dependence on temperature within certain temperature range, which was beneficial and critical for its application under temperature vibration environment. For example, Steffen Uhlig et al. found that nickel doped hydrogenated amorphous carbon films exhibited high GFs up to 30, and their temperature coefficients of resistance (TCR) were just in the range of -300-0 ppm/K [7].

In addition, a-C films also have some definite advantages in consideration of the fabrication processes when applied in MEMS sensors. The preparation processes of a-C films are mature, flexible and compatible with current piezo-resistive MEMS technology, which involves ion beam deposition, DC/RF magnetron sputtering, plasma enhanced chemical vapor deposition and many others [8–10]. Moreover, the fabrication of a-C sensors is safe and green, since no ion implantation process is involved, where the use of dangerous gases like BF_3, AsH_3 or PH_3 is inevitable. Compared with

* Corresponding author.
** Corresponding author at: Key Laboratory of Marine Materials and Related Technologies, Zhejiang Key Laboratory of Marine Materials and Protective Technologies, Ningbo Institute of Materials Technology and Engineering, Chinese Academy of Sciences, Ningbo, 315201, China.
E-mail addresses: zhq0919@xjtu.edu.cn (Q. Zhang), aywang@nimte.ac.cn (A. Wang).
[1] Xin Ma and Xiaoshan Tong contributed equally to this work.

https://doi.org/10.1016/j.sna.2019.111700
0924-4247/© 2019 Elsevier B.V. All rights reserved.

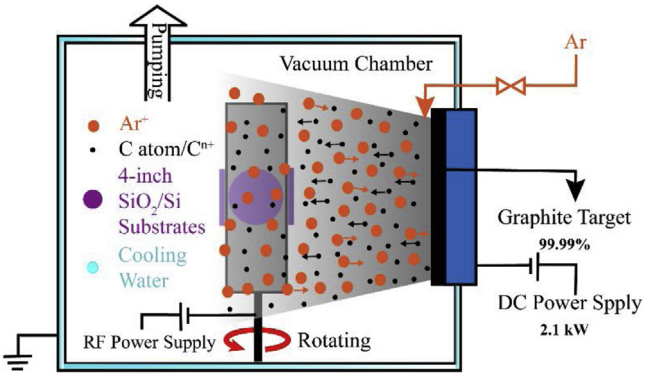

Fig. 1. Schematic diagram of the DC magnetron sputtering for deposition of a-C film.

other promising piezo-resistive materials, such as graphene [11], CNTs [12], silicon nanowires [13,14], a-C film can be easily in-situ deposited on various substrates without complicated transfer process, such as silicon, kinds of metallic substrates and flexible substrates [15–17], which means simple and highly effective fabrication process when it is applied in MEMS sensors.

To realize its application in MEMS sensors, many researchers have attempted to fabricate a-C based MEMS sensors and investigate their performance. Recently. A. Tibrewala et al. integrated a-C:H film into a MEMS GF testing structure which could also be used to monitor force signal [18,19]. Wang et al. transferred a-C film onto polyethylene substrate by a lift-off method and fabricated a flexible piezo-resistive sensor [20]. Saskia Biehl et al. deposited a-C:H films onto the surface of a ball bearing ring to fabricate an in-situ sensor to measure the change of stress during working process [21]. And in our former work, a high performance a-C piezo-resistive sensor was reported [22]. However, the design method of proper structure and sensitive circuit for the a-C MEMS sensors is still not mature and systematic, and the testing of the reliability, repeatability, time-drift and temperature-drift is usually ignored, which restrict their practical applications. What's more, in consideration of the high compression stress in a-C films and poor adhesion between a-C and Si [6], it is still a challenge to select proper deposition parameters for fabricating a-C piezo resistors. Finally, the piezo-resistive mechanism of a-C film is still not clear, which also a challenge for the further developing of this promising functional material.

In this work, H-free a-C films were prepared by DC magnetron sputtering, and their piezo-resistive properties and mechanism were discussed. Some necessary mechanical characteristics were characterized or tested to supply fundamental parameters for the design of a-C MEMS sensor. Then, the sensor with a four-beam sensitive structure was systematically designed and fabricated. Finally, the performance of the MEMS sensor, such as sensitivity, repeatability and drift behaviors were investigated and shown.

2. Materials and methods

2.1. Preparation of a-C film

DC magnetron sputtering process was used to deposit a-C films as shown in Fig. 1. Silicon wafers (n-type <100>) with thermal oxide layer on both sides were used as substrate for depositing a-C film, 4-inch wafers for fabricating sensors and other rectangle substrates for testing the film's characteristics. The high purity graphite target (99.99%) was connected with direct current magnetron system (DCMS) and the distance from the substrates to the target was 10 cm. The base pressure of the vacuum chamber was 3×10^{-3} Pa. Before deposition, the substrate was etched and precleaned in Ar^+ plasma glow for 30 min with the substrate bias voltage of -400 V and the working pressure of 1.1 Pa. The Ar gas was introduced to graphite target in a flow rate of 65 sccm during the self-sputtering and film deposition process. And the working pressure was controlled at 0.3 Pa. In these series of experiments, in order to adjust the ratio of sp^2/sp^3 phase content, negative bias voltage was changed from 0 to 400 V with target current 3.0 A. And a-C films deposited at bias of -200 V, was selected for the following fabrication of piezo-resistive sensor. The detailed deposition parameters of a-C films were listed in Table 1.

Table 1
Deposition parameters of a-C films.

Parameters	Values
Substrate bias voltage (V)	0, 100, 200, 300, 400
Depositing time (min)	30
Graphite target current (A)	3.0
Flow rate of Ar (sccm)	65
Pressure (Pa)	0.3
Deposition temperature (°C)	< 50
Target to substrate distance (cm)	10
Substrate holder rotation rate (rpm)	6

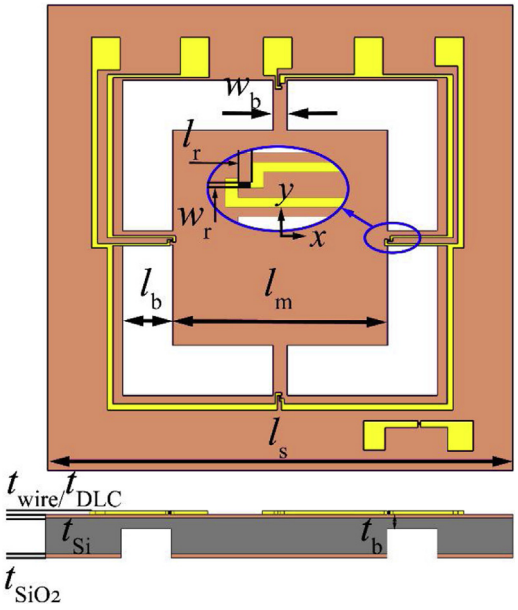

Fig. 2. The schematic diagrams of the a-C piezo-resistive sensor from the top view and cross-sectional view.

After deposition, the thickness of deposited a-C films was tested by profilometer (Alpha-Step IQ) and the value was in the range of 187.4 nm–200.5 nm. This testing result showed that this series of films had good uniformity in thickness.

2.2. Design of the a-C piezo-resistive sensor

In previous reports, to measure the value of applied force, the cantilever [23] and boss-membrane structures [18] were selected for a-C piezo resistors. While, for MEMS piezo-resistive sensors, a Wheatstone full bridge is convenient and commonly used, which can improve the structure sensitivity of the MEMS sensors, so a four-beam structure was selected in this work.

As shown in Fig. 2, the full size of the a-C piezo-resistive sensor was 6.5 mm × 6.5 mm × 0.5 mm, whose structure consisted of four beams, a mass and frame. Four a-C piezo-resistors respectively distributed in the region of stress concentration of each beam, and they formed a Wheatstone full-bridge by the connection of wires. For the

Table 2
Structure parameters of the sensor.

Parameter	value	Parameter	Value
l_s (length and width of the sensor)	6.5 mm	t_{SiO2} (thickness of the SiO_2 film)	300 nm
l_m (length and width of the mass)	3 mm	t_{wire} (thickness of the wire)	220 nm
l_b (length of the beam)	700 μm	$t_{a\text{-}C}$ (thickness of the a-C film)	200 nm
w_b (width of the beam)	200 μm	t_{Si} (thickness of the substrate)	500 μm
		t_b (thickness of the beam)	150 μm

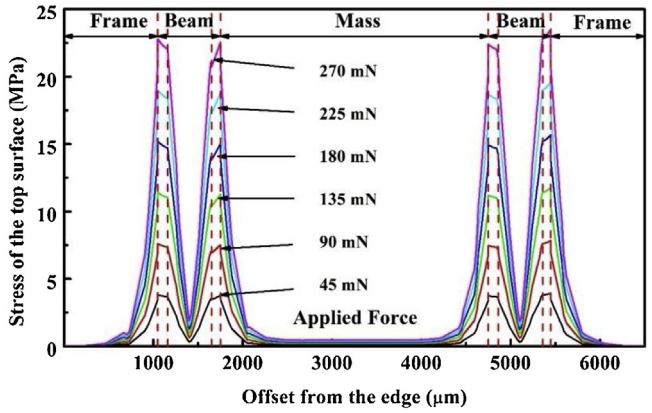

Fig. 3. The simulation result of the distribution of the stress along the X/Y axes.

convenience of fabrication, the structure parameters of sensor were determined as shown in Table 2.

Generally, the piezo-resistors should be set on the regions of stress concentration to obtain high sensitivity of the MEMS sensor, and to confirm the location of the stress concentration area is one key factor. In this work, those regions were determined by mechanical calculation and finite element method (FEM).

When applying a static force on the center of the mass surface, the maximum stress of the structure would appear on the beams' two edges that connected with the frame or mass [24]. Here, the stress concentration regions and the sensitivity of the sensor were further determined with the help of COMSOL Multiphysics software. Due to the symmetrical four-beam sensitive structure of the MEMS sensor, only the location of the stress concentration regions along X/Y axes were determined. As shown in Fig. 3, when the applied force increased from 0 to 270 mN, the corresponding stress curves of different positions also increased. Apparently, the stress concentration regions located at the two edges of each beam, which connected with the frame or mass, and the lengths of the regions varied from 80 to 100 μm, as shown by the distance between two dot lines in Fig. 3. In this work, the length of the piezo-resistors (l_r) was 40 μm, and the width of the resistors (w_r) was 20 μm, which was much smaller than the width of beam (w_b).

Different from single crystal silicon, a-C film was an isotropic material, which caused problems in the sensitive circuit design of the sensor. Therefore, the piezo-resistive effect module of COMSOL Multiphysics software was employed to assist the electrical design of the a-C piezo-resistive MEMS sensor, and boundary-current model was used in this FEM simulation. Here, the piezo resistive material setting of a-C film derived from the internal material p-silicon (single-crystal, lightly doped). Some parameters the of a-C film were specified in the software, its density was 2800 kg/m^3 measured by X-ray reflectivity (XRR) method (D8 DISCOVER, Bruker), and Young's modulus was between 170.2–185.2 by nano-indentation test (G200, MTS).

Not like silicon, a-C film has an amorphous inner structure that caused an isotropic performance, and the GF of it determined by the 3-point method was a coupled value from all principle and shear strain directions [7,25]. What's more, as shown in Fig. 4(a) and (b), only stress along X and Y direction played main role. Referring to the piezo resistive coefficient matrix of p-silicon, in the model of a-C film, Eq. (1) can be used for the piezo resistive calculation, where k is the GF of a-C film and k_x=k_y=k, additionally, k=πE.

$$\frac{\Delta\rho}{\rho}E = k_x\sigma_x + k_y\sigma_y \tag{1}$$

$$\pi = \begin{pmatrix} k_x/E & 0 & 0 & 0 & 0 & 0 \\ 0 & k_y/E & 0 & 0 & 0 & 0 \\ 0 & 0 & 0 & 0 & 0 & 0 \\ 0 & 0 & 0 & 0 & 0 & 0 \\ 0 & 0 & 0 & 0 & 0 & 0 \\ 0 & 0 & 0 & 0 & 0 & 0 \end{pmatrix} \tag{2}$$

Then, in this work, the FEM electrical simulation was executed based on Eq. (1) and the piezo resistive coefficient of p-silicon was rewritten into Eq. (2). In addition, a Wheatstone full-bridge circuit was applied in this a-C piezo-resistive sensor to improve the sensitivity.

2.3. Fabrication of the a-C piezo-resistive sensor

Fig. 5 presents the fabrication process of the a-C piezo-resistive sensor. In this work, 4-inch silicon substrates (n-type <100 >) were directly used to fabricate a-C piezo-resistive sensors. And in order to obtain high electrical insulation property, the silicon substrates were modified by thermal oxidization to grow 300 nm SiO_2 on both sides. The patterning for a-C piezo resistors was based on lift-off process [23]. For the working temperature during the deposition process of a-C was under 50 °C, photoresist was directly used as mask for a-C piezo-resistive resistors to simplify the sensor's fabrication processes as shown in Fig. 5(a). In Fig. 5(b), after depositing a-C, the photoresist mask was removed by ultrasonic process using acetone for 10 min and then a-C film was patterned into piezo-resistors.

Then 20 nm Cr and 200 nm Au films were successively deposited to make lead wires by lift-off process, which was shown in Fig. 5(c). As shown in Fig. 5(d) and (e), for the fabrication of the backside structure, inductively coupled plasma (ICP) etching process after 300 nm Al mask was sputtered on backside. And the thickness of the remaining diaphragm was kept around 150 ± 10 μm. Using the same process, the four-beam structures were released, as shown in Fig. 5(f) and (g). After the etching of the Al mask, the force sensor chips were cleaned by acetone and deionized water. Finally, laser cutting was used for scribing.

The sensor chips after scribing were shown in Fig. 6(a). The chip was adhered to custom-made print circuit board (PCB) by epoxy resin and electrical connection was established by using wire bonding and soldering, which was shown in Fig. 6(b). The inset picture in Fig. 6(b) showed the good connection between a-C and Au/Cr wires after all processes.

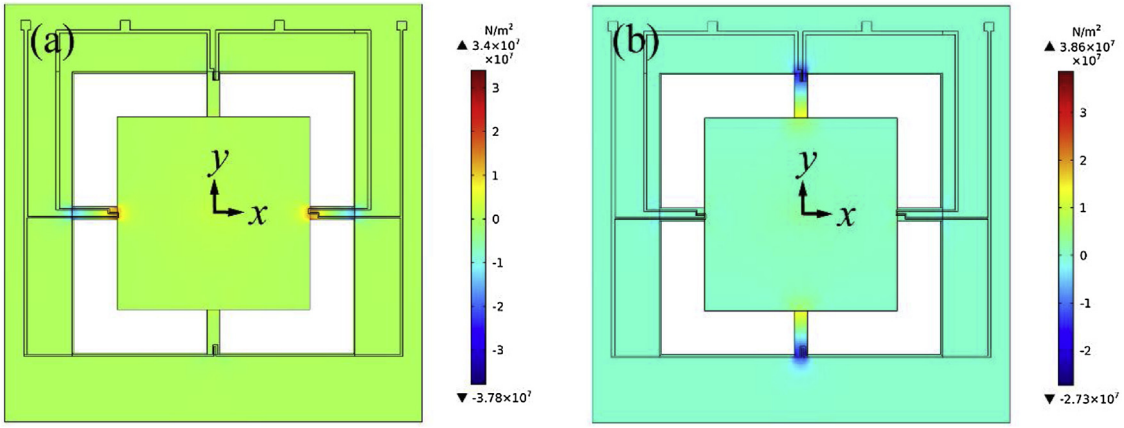

Fig. 4. The nephograms of the principle stress along X (a), and Y direction (b).

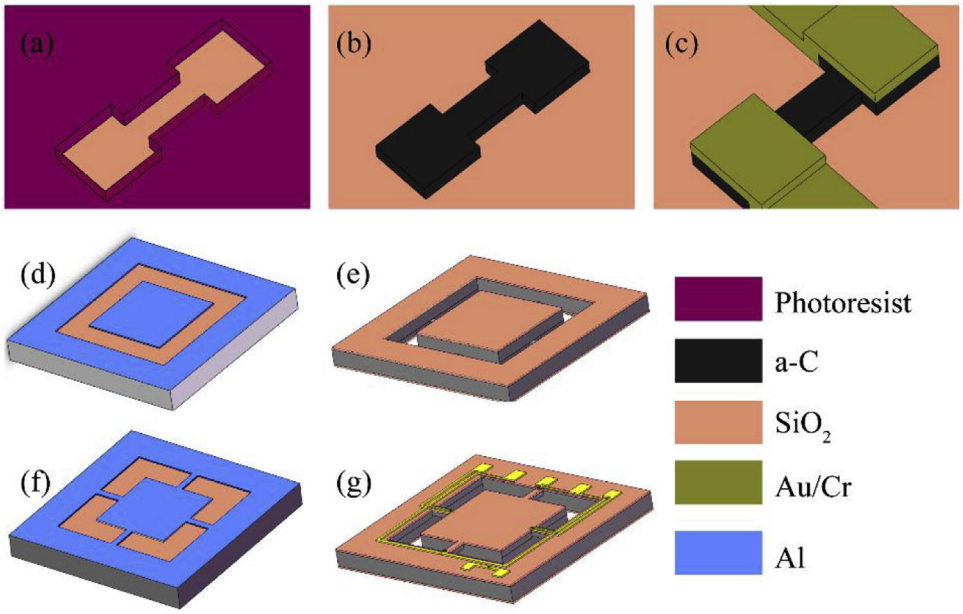

Fig. 5. Schematic of the fabrication process of a-C piezo-resistive sensor, preparing photoresist mask for a-C piezo resistors (a), deposition of a-C film and removing mask by lift-off process (b), making lead wires (c), making backside Al mask (d), fabricating the back structure by ICP etching (e), making front side Al mask (f), fabricating the front structure by ICP etching (g).

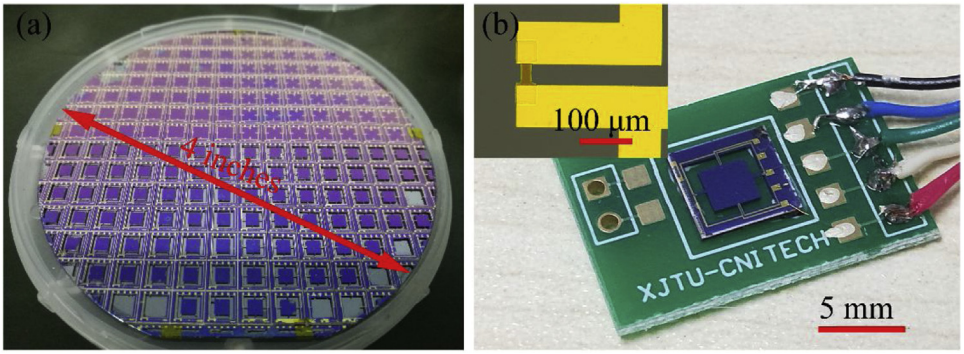

Fig. 6. Silicon wafer after fabrication process (a), a-C piezo-resistor and piezo-resistive sensor after packaging (b).

2.4. Characterization methods of a-C film and sensor

Scanning electron microscopy (SEM, Hitachi S4800) was applied to observe the morphology of the a-C films. Atomic force microscope (AFM, Bruke INNOVA) was used for surface profile and Conductive AFM (CAFM) test. Raman spectra (LabRAM HR Evolution, HORIBA) equipped with a laser of 532 nm exciting wavelength was used to evaluate the sp^2 cluster size and other characters of film. The thickness of deposited a-C films was tested by profilometer (Alpha-Step IQ). Scratch tester (CSM Revetest scratch tester)

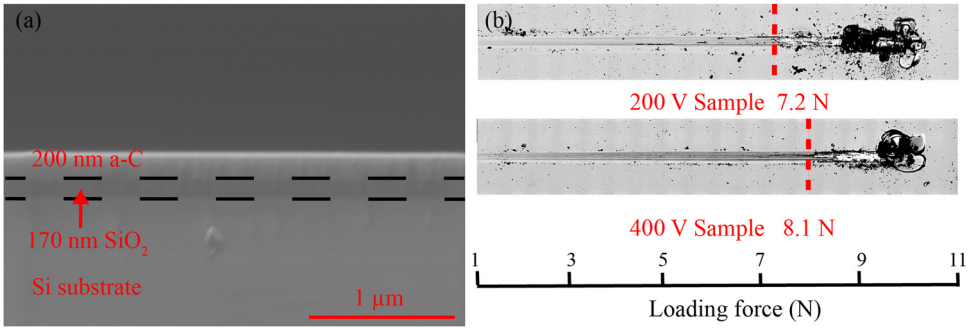

Fig. 7. Cross-section morphology of a-C film and the substrate (a), the image of the samples after the scratch test (b).

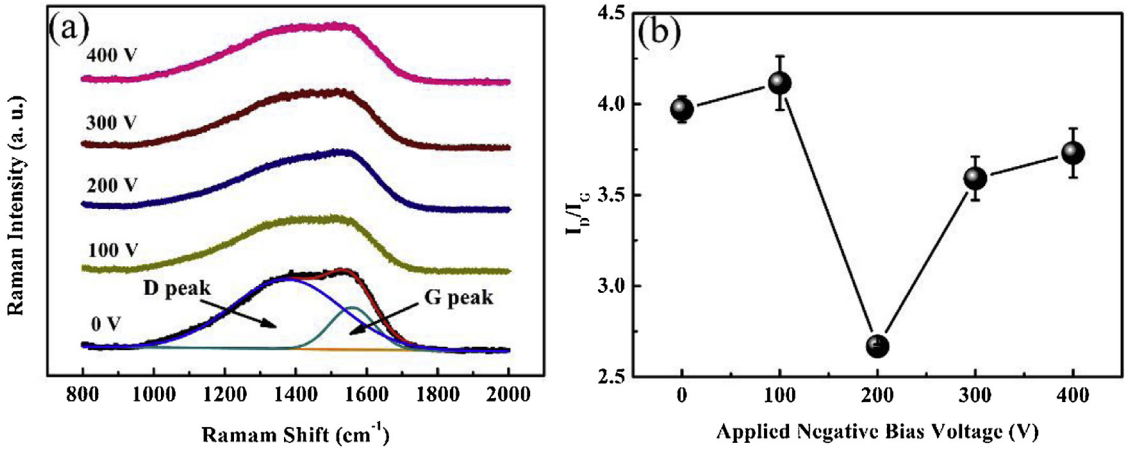

Fig. 8. Raman spectra of the a-C films (a), the correlation between fitted value of I_D/I_G and negative bias voltage (b).

was used to test the adhesion force between the film and substrate. The GF of the a-C films were measured by home-made three-point testing device. In the sensors' testing, analytical balance (XS105 DU, Mettler Toledo) was used to measure the applied force and desktop multimeter (Fluke 8846A) was used to record the electric signals. The temperature dependence of a-C film and the sensor's temperature drift was separately tested in the temperature range from -20 °C to 150 °C and 20 °C to 60 °C in oven (PSL-2 J, Espec).

3. Results and discussion

3.1. The property of a-C film

Fig. 7(a) showed the SEM image of the cross-section morphology of a-C film deposited on SiO_2/Si. The a-C film was about 200 nm with smooth cross-section morphology, and the interface between a-C and SiO_2 was clear and no significant peeling occurred. From the point of practical application, enough adhesion strength between the a-C film and SiO_2/Si substrate was the guarantee for the fabrication and the good stability of the sensor. So, its adhesion strength was evaluated by scratch test, with an optical microscope used to evaluate the critical force-L_{c3} (spallation inside the groove) [26]. At least three tests were taken for each sample to determinate the average adhesion force. As shown in Fig. 7(b), the value of L_{c3} was 7.2 N for sample deposited at 200 V and 8.1 N at 400 V. What's more, the a-C film did not peel off from the Si substrates during the following sensor fabrication process.

Fig. 8 displays the Raman spectra of a-C films. All the Raman spectra showed a typical broad characteristic of a-C in wavelength from 800 to 2000 cm^{-1}. For the a-C, the broad peak can be designated to D peak at 1380 cm^{-1} and G peak at 1552 cm^{-1}. The D peak is due to the breathing mode of sp^2 atoms in rings, while the G peak is due to the stretching mode all pairs of sp^2 atoms in both rings and chains. Empirically, the sp^2/sp^3 ration and the size of sp^2 cluster can be qualitatively discussed from the position of G peak, intensity ratio of D peak to G peak (I_D/I_G) [27]. In Fig. 8, from 0 V to 100 V, similar values of I_D/I_G were obtained; then, I_D/I_G decreased obviously along with the change of bias voltage from 100 V to 200 V; from 200 V to 300 V, I_D/I_G increased up to 3.59 and then remained stable when bias voltage was changed to 400 V. This result indicted that the sp^2 cluster size in the a-C films was successfully regulated by changing the bias voltage.

The gauge factor (GF) of the a-C films was tested by a home-made three-point method device. Fig. 9(a) shows the testing device, which consists of the test sample, 3D printed holder, dial gauge and the loading mechanism. The samples were cut into rectangles with the dimension of 35 mm × 5 mm × 0.5 mm, and they could be approximated to the simply supported beam model when force was applied. By turning the hand wheel of the loading mechanism, the indenter will be drived downwards to touch and push the samples, and the force and deformation can be applied. The initial resistance and resistance under certain force were recorded when the indenter contacted the center of the samples. During the subsequent loading process, the change of vertical position of the indenter (ΔY) and the change of resistance (ΔR) was measured by dial gauge and multimeter, respectively. The thickness (t) of the samples was 500 ± 10 μm and the distance between the two support points (l) was restricted by the 3D printed holder. Then the gauge factor (K) was calculated by Formula 4 [28]:

$$K = \frac{l^2}{3t \cdot \Delta Y} \cdot \frac{\Delta R}{R_0} \tag{4}$$

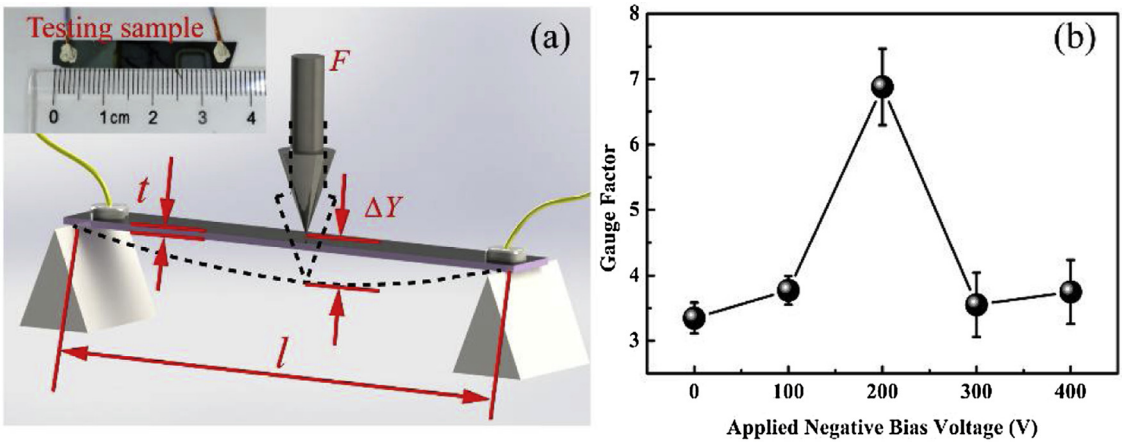

Fig. 9. The 3-D schematic of homemade gauge factor testing device and the photograph of testing sample (a), GF testing result (b).

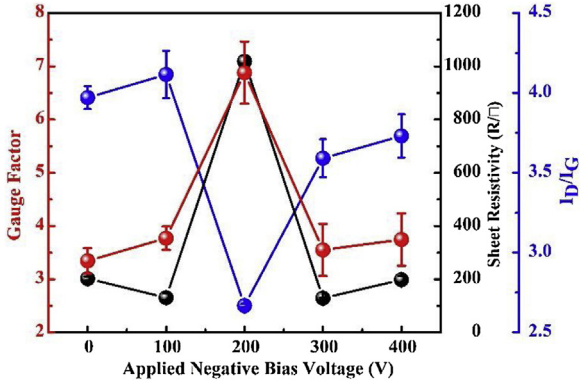

Fig. 10. The GF, I_D/I_G, and sheet resistivity of a-C films at various biases.

Fig. 9 shows the value of GF at various bias voltages. In the range from 0 to 400 V, the GF of the films were between 3.3 to 6.9, increasing bias voltage from 0 to 100 V, the GF kept nearly constant; when the bias voltage rose up to 200 V, the GF evidently increased; from 200 V to 300 V, the GF decreased quickly; then from 300 V to 400 V, the GF remained nearly unchanged. Though an obvious irregular evolution of GF was observed with the change of bias voltage, it still proved that GF of a-C films could be successful adjusted by changing the bias voltage.

Fig. 10 exhibited the relation between the GF, value of I_D/I_G and sheet resistivity of the films. Regardless of the bias voltage, the GF of the films showed distinct relevance with I_D/I_G and sheet resistivity. That was, smaller sp^2 cluster size or larger sheet resistivity corresponded to larger GF. That experimental result indicated that the relation between GF, I_D/I_G and sheet resistivity might coincide with thick film resistors theory [19,29], which is used to explain the origination of the piezo-resistive effect of a-C film. In this theory, the a-C film can be described as a composite of conductive sp^2 clusters that are only a few nanometers in an insulating sp^3 matrix, and carriers transport between clusters by tunneling [30]. When force is applied to a-C films, the distance between conductive sp^2 clusters changes and hence the thickness of insulating layer changes, which causes change of resistivity at the macro level. However, the mechanism of this effect shows its complexity when several related works were compared. The resistivity of a-C film was between several hundred ohm to several megohm per sheet according to the work of Š. Meškinis et al. [31], but the GF was only in the range of 4-16. While in the work of E. Peiner et al, the resistivity was about 2–4 kΩ/□, which corresponded to the GF of 17–32 [32]. Moreover, in this work, for the samples with larger size of sp2 cluster, they exhibiting smaller GF and sheet resistivity which was in 200–400 Ω/□. For the sample deposited at −200 V, the GF was 6.9 while the sheet resistivity was nearly 1 000 Ω/□. Therefore, more work is urgent needed to build the mechanism model.

Furtherly, in this work, to prove that the model based on sp^2 clusters and sp^3 matrix was applicable, CAFM test was employed since it could be used to evaluate the nanoscale electron conducting properties. As shown in the following Fig. 11(a) and (b), Cr film of 200 nm was pre-deposited on silicon substrate as bottom electric contact, then a-C film was deposited, finally the conductive silver paste was used as wires between a-C film and the conductive substrate. Before CAFM testing, the surface profile was tested using tapping mode as shown in Fig. 11(c). For the Cr layer had large grain, the roughness of the sample increased obviously. Fortunately, the 2-D dimension of the grains was in the range of dozens of nanometer to 100 nm, which was much bigger than the size of sp^2 clusters. Therefore, these grains would not affect the test in this work. In Fig. 11(d), the 3-D image showed obvious difference in electrical conductivity of the a-C film, which could be used to qualitatively identify different phases [33,34]. According to the CAFM test results shown in Fig. 11(e)–(h), some light parts were distributed (highly conductive) in the surface image, since sp^2-C showed larger conductivity than that of sp^3-C, which could reflect the distribution of sp^2 clusters in the sp^3 matrix to some extent.

3.2. The performance of a-C force sensor

The performance of the a-C force sensor was systematically tested. Due to its highest GF, the a-C film deposited at -200 V was used for the design and fabrication of sensor. In Fig. 11(a), the packaged sensor was pasted on the platform of analytical balance. And right above the geometric center of the mass, a pinhead was used for applying force to the sensor, which was driven by a lead-screw mechanism.

First, the sensitivity and repeatability of the a-C sensor were tested in the force range of 0–210 mN. As shown in Fig. 12(b), the sensitivity of the force sensor was 9.8 μV/V/mN and the nonlinearity was 2.0% FS during loading procedure and 2.2% FS during unloading procedure. The FEM simulation result was also present and it matched the real signal well, which confirmed the validity of the simulation method mentioned above. To investigate the reliability and repeatability of the a-C piezo-resistive sensor, 100 tests under cyclic loading were performed. And highly linear offset signals of Wheatstone full-bridge can be observed during each test, and no obvious variation of the offset signals can be detected after the cyclic test, which exhibited a good reliability and high repeatability of the sensor, as shown in Fig. 12(c).

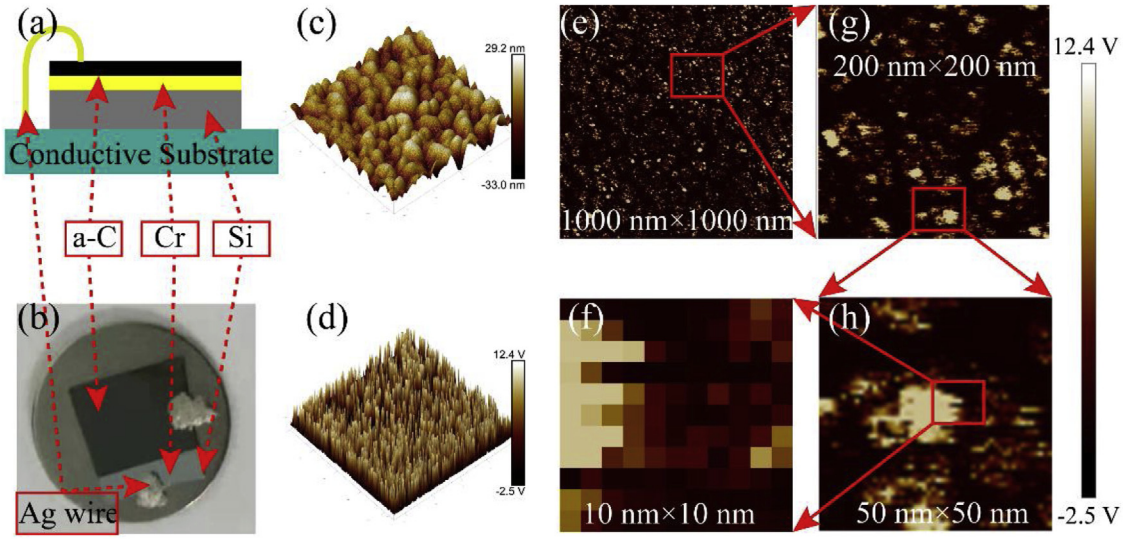

Fig. 11. Illustration and results of CAFM test, the structure of a-C sample (a), the photo of the sample (b), height result of the sample (c), 3-D CAFM result (d), 2-D CAFM results (e)-(h), the scale for them was shown on the right.

Table 3
Piezo resistive performances of several a-C sensors.

Authors of related works	Structure and structural sensitivity	Key dimension of sensor	Gauge factor in sensors	Sensor's sensitivity (or transformed as $\Delta R/R/F$)
E. Peiner et al. [32]	Boss-membrane/higher	49 ± 3 μm (thickness of membrane)	$17 \pm 3/32 \pm 5$	1.2% N^{-1}/1.9% N^{-1}
Xin Ma et al. [22]	Flat membrane/low	170 ± 10 μm (thickness of membrane)	7.1	0.0081% N^{-1}
This work	Four-beam-mass/high	150 ± 10 μm (thickness of beams)	6.9	1% N^{-1}
E. Peiner et al. [23]	Cantilever/highest	50 μm (thickness of cantilever)	36-46	220-313% N^{-1}
E. Peiner et al. [35]	Boss-membrane/high	50 μm (thickness of membrane)	Unknown	134 ± 11 μV/μm52 ± 1 μV/μm

Then, from the point of practical application, the time-drift and temperature-drift of the sensor were respectively measured for 60 min and within the temperature range from 20 °C to 60 °C with a 10 °C interval. The results were shown in Fig. 12(d) and (e) respectively.

The time drift of the sensor was only within ±0.15 mV. As to its temperature-drift property, the zero-offset voltage of a-C sensor decreased with the increase of temperature, which was caused by the initial unbalance of Wheatstone full-bridge and the resistivity change of the a-C piezo resistors. In order to evaluate the a-C piezo resistor's temperature-conductivity relation more precisely, an oven was used to provide a changing temperature environment. And Fig. 13 shows the relation between the its resistivity of a-C film deposited at -200 V and the test temperature from −20 °C to 150 °C. The resistivity of the a-C film decreased linearly with the increased of temperature and this relation could be fitted by

$$\rho(\times 10^{-4}) = 2.5089 - 0.00424T, \quad (5)$$

where ρ is the resistivity of a-C piezo resistor, T is the temperature in centigrade degree. Though this characteristic of a-C film may bring temperature drift to the MEMS force sensor, the non-linearity is only 3.1% FS, so it is still beneficial and easy for researchers to make temperature compensation for further application.As shown in Table 3, the sensor's performance bases both on their structural and sensitive material sensitivity. Nowadays, several classic sensitive structures in MEMS piezo resistive sensors have been applied in a-C sensors, which shows the good compatibility of a-C film in MEMS sensors. What's more, in this work, the sensitivity, non-linearity, repeatability, time and temperature drift were systematically tested and shown, which also shows this sensitive material's feasibility for practical application in MEMS piezo resistive sensors.

4. Conclusion

In this paper, a systematic method for studying the piezo-resistive performance of a-C film and developing piezo-resistive sensor based on it was shown. A series of a-C films deposited under different negative bias voltages were characterized. From the Raman spectra analysis result, an obviously connection between the GF, sp^2 cluster size and sheet resistivity was found, which contributed to TFRs theory. Then the mechanical and electrical behaviors of a-C film were used for the design and FEM simulation for the sensor. After economical fabrication process, the sensitivity of the force sensor was 9.8 μV/V/mN. Moreover, the sensor showed a very good repeatability, which was necessary for the practical application. This work contributed to the wide application of a-C film in MEMS sensors and the more economical, efficient and environmentally friendly piezo-resistive component fabrication process.

Declaration of Competing Interest

Xin Ma the piezo-resistive mechanism of a-C film, piezo-resistive MEMS sensors.

Xiaoshan Tong piezo-resistive MEMS pressure sensor.

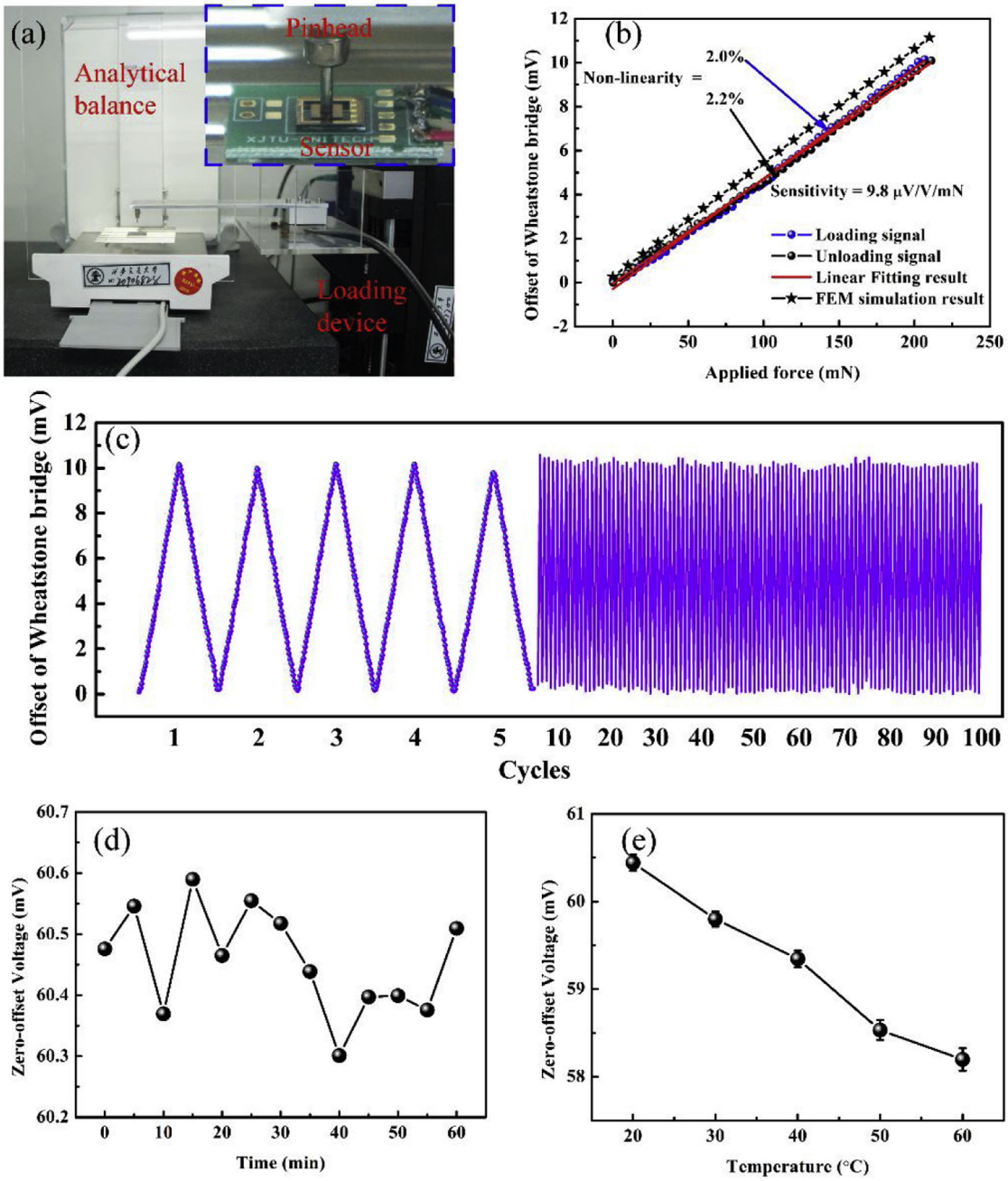

Fig. 12. Testing system for a-C force sensor (a), the real and FEM simulated offset signals of Wheatstone full-bridge under loading and unloading procedure (b), result of repeatability testing (c), the time-drift of the sensor (d), the temperature-drift of the sensor (e).

Peng Guo preparation, characterization and electrical properties of amorphous carbon films.

Yulong Zhao MEMS sensors, micro and nano fabrication.

Qi Zhang the piezo-resistive mechanism of Graphene, MoS_2 and a-C film, MEMS sensors.

Hanchao Li tetrahedral amorphous carbon and the conversion of amorphous carbon to graphene.

Rende Chen vacuum technologies and plasma diagnosis.

Aiying Wang advanced carbon-based materials, materials simulation, plasma surface engineering, and so on.

Acknowledgments

This research was supported by the National Nature Science Foundation of China (51805425, U1505244, 51602319), the National Nature Science Foundation of Shaanxi Province (2018JQ5018), the Ningbo Science and Technology Innovation Project (2018B10014), and the Fundamental Research Funds for the Central Universities (xzy022019038, xjj2018046).

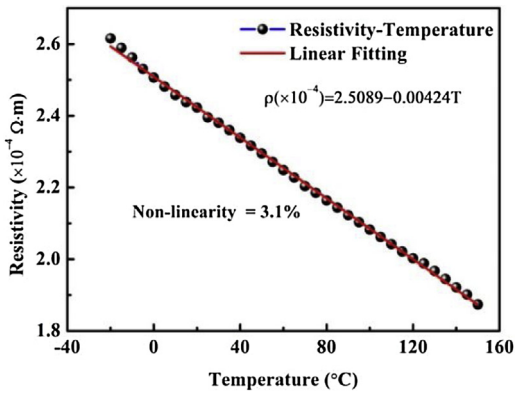

Fig. 13. The relation between the a-C piezo resistor's conductivity and the temperature.

References

[1] J. Robertson, Diamond-like amorphous carbon, Mater. Sci. Eng. R. 37 (2002) 129–281.
[2] A. Sebastian, A. Pauza, C. Rossel, R.M. Shelby, A.F. Rodríguez, H. Pozidis, et al., Resistance switching at the nanometre scale in amorphous carbon, New J. Phys. 13 (2011), 013020.
[3] P. Guo, R. Chen, L. Sun, X. Li, P. Ke, Q. Xue, et al., Bulk-limited electrical behaviors in metal/hydrogenated diamond-like carbon/metal devices, Appl. Phys. Lett. 112 (2018), 033502.
[4] S.N. Meskinis, R. Gudaitis, K. Slapikas, A. Vasiliauskas, A. Ciegis, T. Tamulevicius, et al., Giant negative piezoresistive effect in diamond-like carbon and diamond-like carbon-based nickel nanocomposite films deposited by reactive magnetron sputtering of Ni target, ACS Appl. Mater. Interfaces 10 (2018) 15778–15785.
[5] A. Tibrewala, E. Peiner, R. Bandorf, S. Biehl, H. Lüthje, Transport and optical properties of amorphous carbon and hydrogenated amorphous carbon films, Appl. Surf. Sci. 252 (2006) 5387–5390.
[6] M. Petersen, R. Bandorf, G. Bräuer, C.P. Klages, Diamond-like carbon films as piezoresistors in highly sensitive force sensors, Diam. Relat. Mater. 26 (2012) 50–54.
[7] S. Uhlig, H. Schmid-Engel, T. Speicher, G. Schultes, Pressure sensitivity of piezoresistive nickel–carbon Ni:a-C:H thin films, Sens. Actuators A-Phys. 193 (2013) 129–135.
[8] L. Liu, T. Wang, J. Huang, Z. He, Y. Yi, K. Du, Diamond-like carbon thin films with high density and low internal stress deposited by coupling DC/RF magnetron sputtering, Diam. Relat. Mater. 70 (2016) 151–158.
[9] K.C. Park, J.H. Moon, J. Jang, M.H. Oh, Deposition of hydrogen-free diamond-like carbon film by plasma enhanced chemical vapor deposition, Appl. Phys. Lett. 68 (1996) 3594–3595.
[10] S. Srinivasan, Y. Tang, Y.S. Li, Q. Yang, A. Hirose, Ion beam deposition of DLC and nitrogen doped DLC thin films for enhanced haemocompatibility on PTFE, Appl. Surf. Sci. 258 (2012) 8094–8099.
[11] A.D. Smith, F. Niklaus, A. Paussa, S. Schroder, A.C. Fischer, M. Sterner, et al., Piezoresistive properties of suspended graphene membranes under uniaxial and biaxial strain in nanoelectromechanical pressure sensors, ACS Nano 10 (2016) 9879–9886.
[12] H.R. Khalid, I.W. Nam, I. Choudhry, L. Zheng, H.K. Lee, Piezoresistive characteristics of CNT fiber-incorporated GFRP composites prepared with diversified fabrication schemes, Compos. Struct. 203 (2018) 835–843.
[13] R. He, P. Yang, Giant piezoresistance effect in silicon nanowires, Nat. Nanotechnol. 1 (2006) 42–46.
[14] K. Winkler, E. Bertagnolli, A. Lugstein, Origin of anomalous piezoresistive effects in VLS grown Si nanowires, Nano Lett. 15 (2015) 1780–1785.
[15] S. Miyake, S. Yamazaki, Evaluation of protuberance and groove formation in extremely thin DLC films on Si substrates due to diamond tip sliding by atomic force microscopy, Wear 318 (2014) 135–144.
[16] D.J. Li, F.Z. Cui, H.Q. Gu, W.Z. Li, Ion beam-assisted deposition of DLC films on PMMA and TiN/PMMA, Vacuum 56 (2000) 205–211.
[17] H.W. Choi, K.-R. Lee, R. Wang, K.H. Oh, Fracture behavior of diamond-like carbon films on stainless steel under a micro-tensile test condition, Diam. Relat. Mater. 15 (2006) 38–43.
[18] A. Tibrewala, E. Peiner, R. Bandorf, S. Biehl, H. Lüthje, Piezoresistive gauge factor of hydrogenated amorphous carbon films, J. Micromech. Microeng. 16 (2006) S75–S81.
[19] A. Tibrewala, E. Peiner, R. Bandorf, S. Biehl, H. Lüthje, Longitudinal and transversal piezoresistive effect in hydrogenated amorphous carbon films, Thin Solid Films 515 (2007) 8028–8033.
[20] B. Wang, Y.C. Jiang, R. Zhao, G.Z. Liu, A.P. He, J. Gao, Piezoresistive effect observed in flexible amorphous carbon films, J. Phys. D Appl. Phys. 51 (2018), 175304.
[21] S. Biehl, H. Lüthje, R. Bandorf, J.-H. Sick, Multifunctional thin film sensors based on amorphous diamond-like carbon for use in tribological applications, Thin Solid Films 515 (2006) 1171–1175.
[22] X. Ma, P. Guo, X. Tong, Y. Zhao, Q. Zhang, P. Ke, et al., Piezoresistive behavior of amorphous carbon films for high performance MEMS force sensors, Appl. Phys. Lett. 114 (2019).
[23] E. Peiner, A. Tibrewala, R. Bandorf, S. Biehl, H. Lüthje, L. Doering, Micro force sensor with piezoresistive amorphous carbon strain gauge, Sens. Actuators A-Phys. 130-131 (2006) 75–82.
[24] P. Wang, Y. Zhao, B. Tian, Y. Liu, Z. Wang, C. Li, et al., A piezoresistive micro-accelerometer with high frequency response and low transverse effect, Meas. Sci. Technol. 28 (2017).
[25] N.D. Madsen, J. Kjelstrup-Hansen, Three-point bending setup for piezoresistive gauge factor measurement of thin-film samples at high temperatures, Rev. Sci. Instrum. 88 (2017), 015001.
[26] M. Jelínek, P. Písařík, T. Kocourek, J. Zemek, J. Lukeš, Influence of ion bombardment on growth and properties of PLD created DLC films, Appl. Phys. A-Mater. 110 (2012) 943–947.
[27] A.C. Ferrari, J. Robertson, Interpretation of Raman spectra of disordered and amorphous carbon, Phys. Rev. B 61 (2000) 14095–14107.
[28] Y.L. He, X.H. Wu, H.Y. Lin, H. Wang, C. Li, Structure characteristics and piezoresistive effect of nc-Si:H films, Chin. Sci. Bull. 40 (1995) 1684–1687.
[29] C. Grimaldi, P. Ryser, S. Strässler, Gauge factor enhancement driven by heterogeneity in thick-film resistors, J. Appl. Phys. 90 (2001) 322–327.
[30] G. Ambrosetti, I. Balberg, C. Grimaldi, Percolation-to-hopping crossover in conductor-insulator composites, Phys. Rev. B 82 (2010).
[31] Š. Meškinis, A. Vasiliauskas, K. Šlapikas, R. Gudaitis, S. Tamulevičius, G. Niaura, Piezoresistive properties and structure of hydrogen-free DLC films deposited by DC and pulsed-DC unbalanced magnetron sputtering, Surf. Coat. Technol. 211 (2012) 172–175.
[32] E. Peiner, A. Tibrewala, R. Bandorf, H. Lüthje, L. Doering, W. Limmer, Diamond-like carbon for MEMS, J. Micromech. Microeng. 17 (2007) S83–S90.
[33] H. Fan, D. Yang, L. Sun, Q. Yang, J. Niu, Z. Bi, et al., Structural and electrical evolution of He ion irradiated hydrocarbon films observed by conductive atomic force microscopy, Nucl. Instr. Methods Phys. Res. Sect. B-Beam Interactions Mater. Atoms 312 (2013) 90–96.
[34] F. Hui, M. Lanza, Scanning probe microscopy for advanced nanoelectronics, Nat. Electron. 2 (2019) 221–229.
[35] E. Peiner, A. Tibrewala, R. Bandorf, S. Biehl, H. Lüthje, L. Doering, Mechanical and piezoresistive properties of diamond-like carbon for MEMS, in: T. Gessner (Ed.), Proc Intern Conf Smart Systems Integration 2007, VDE-Verlag, Paris, France, 2007, pp. 257–264.

Biographies

Xin Ma received the bachelor's degree in mechanical mechanism, Xi'an Jiaotong University, China, in 2016. Thereafter he joined Zhao Yulong's group as an integrated Ph.D. student in 2016. His interests are the piezo-resistive mechanism of a-C film, piezo-resistive MEMS sensors.

Xiaoshan Tong received the bachelor's degree in mechanical mechanism, Northwestern Polytechnical University, China, in 2017. Thereafter she joined Zhao Yulong's group as a master student in 2017. Her interest is the piezo-resistive MEMS pressure sensor.

Peng Guo received the Ph.D. degree in materials physics and chemistry, University of Chinese Academy of Sciences, China, in 2015. He is now the associate professor in Ningbo Institute of Materials Technology and Engineering, Chinese Academy of Sciences. His research interest covers preparation, characterization and electrical properties of amorphous carbon films.

Yulong Zhao received the Ph.D. degree in Mechanical Engineering from Xi'an Jiaotong University, China, in 2003. He is now the professor in Xi'an Jiaotong University, and the associate director of State Key Laboratory for Manufacturing Systems Engineering of Xi'an Jiaotong University, China. He also obtained the Changjiang Scholar and the National Outstanding Youth Funds, China. His research interest covers MEMS sensors, micro and nano fabrication.

Qi Zhang received the Ph.D. degree in Mechanical Engineering from Xi'an Jiaotong University, China, in 2014. She is now the teacher in Xi'an Jiaotong University. Her research interest covers the MEMS sensors, piezo-resistive mechanism of new materials, such as Graphene, and a-C film.

Hanchao Li received the bachelor degree in Materials Chemistry from Wuhan Institute of Technology, China, in 2015. Now, he is a **Ph.**D. student at ShanghaiTech University in China. In addition, he is a postgraduate cooperation with Ningbo

Institute of Materials Technology and Engineering co-cultured. His research interest is tetrahedral amorphous carbon and the conversion of amorphous carbon to graphene.

Rende Chen received the B.S. degree in communication engineering from the Beijing Institute of Petrochemical Technology, Beijing, China, in 2010, and the M.S. degree in material science and engineering from the University of Chinese Academy of Sciences, Beijing, China. He is currently with the Ningbo Institute of Material Technology and Engineering, Chinese Academy of Sciences, Ningbo, China, where he is involved in the research work. His current research interests include vacuum technologies and plasma diagnosis.

Aiying Wang received the B.S. degree in material science and engineering from Northwestern Polytechnical University, Xi'an, China, in 1998, and the Ph.D. degree from the Institute of Metal Research, Chinese Academy of Sciences, Shenyang, China, in 2003. Her current research interests include advanced carbon-based materials, materials simulation, plasma surface engineering, and so on.